Int J Cardiovasc Imaging (2011) 27:251–258
DOI 10.1007/s10554-011-9798-1

REVIEW

Intracoronary optical coherence tomography, basic theory and image acquisition techniques

F. Prati · M. W. Jenkins · A. Di Giorgio · A. M. Rollins

Received: 1 January 2011 / Accepted: 8 January 2011 / Published online: 17 February 2011

Abstract Optical coherence tomography (OCT) imaging is showing great potential as an alternative or complementary tool to intravascular ultrasound (IVUS) for aiding in stent procedures and future diagnosis/treatment of atherosclerosis. Here, we describe the basic theory behind OCT imaging and explain important parameters such as axial resolution, lateral resolution and sensitivity. Also, we describe several image acquisition techniques that have been adopted for OCT imaging.

Keywords Optical coherence tomography · Stent procedures · Atherosclerosis · Image acquisition

Introduction

Optical coherence tomography (OCT) is an emerging medical imaging modality capable of in situ imaging of tissue microstructure with micrometer resolution [1–5]. Analogous to ultrasound, OCT noninvasively measures backscattered light returning from a sample in real time. OCT fills a niche in imaging by helping to bridge the gap between cellular imaging modalities, which have less depth penetration compared to OCT (1–2 mm), and full-body imaging systems, which have lower resolution in comparison to OCT (1–15 μm). Also, OCT has the ability to image internal structures in the human body by being implemented with flexible imaging probes such as catheters and endoscopes [6–10]. In particular, OCT has shown great potential in intravascular imaging as an alternative or complementary tool to intravascular ultrasound (IVUS). The robust characteristics of OCT are enabling the imaging modality to become extremely useful in both basic research and clinical applications.

The earliest intravascular OCT studies were ex vivo and demonstrated the ability to image through a coronary catheter [11] and visualize arterial microstructure [12]. As the technology developed further intracoronary OCT imaging was demonstrated in human patients and showed great promise [13, 14]. As compared to IVUS, OCT has much higher resolution (10–15 μm vs. 100 μm), whereas IVUS can image through blood and much deeper into the tissue (2 mm vs. 1 cm). OCT has great promise for aiding in stent procedures, because the position of the stent within the tissue can easily be identified. Also, OCT can identify atherosclerotic plaques with high resolution, which may aid in future diagnosis and treatment of atherosclerosis. This review explains the

F. Prati
Interventional Cardiology, San Giovanni Hospital, Rome, Italy

F. Prati · A. Di Giorgio
CLI Foundation, Viale Bruno Buozzi, 60, Rome, Italy

M. W. Jenkins (✉) · A. M. Rollins
Department of Biomedical Engineering, Case Western Reserve University, Cleveland, OH 44106, USA
e-mail: mwj5@case.edu

theory and image acquisition techniques behind intravascular OCT imaging.

OCT theory

Like IVUS, the typical orientation of OCT images is in cross section. A single depth profile is called an A-scan (see left panel of Fig. 1). By scanning the light beam across the sample, a series of A-scans are captured and together produce a 2-D image called a B-scan (see middle panel of Fig. 1). OCT is capable of producing hundreds of B-scans/second for real time monitoring of even the fastest events [15, 16]. By scanning an area of the sample, 3-D images of the tissue can be constructed (see right panel of Fig. 1). OCT imaging catheters, as used in intravascular imaging,[6, 13] scan the tissue by rotating the catheter for cross-sectional images (B-scans). An automated pullback system allows the catheter to image along the length of the vessel and traces a helical pattern when combined with rotation for 3-D images of the lumen of the vessel. After collecting data from a rotating catheter, a geometrical transform is applied to the data to convert the data from rectangular to polar coordinates.

Unlike ultrasound which directly measures the transit time of sound, OCT measures the interference pattern of the light to discern the depth of a reflector in the sample because light travels too fast to directly detect transit time. An interferometer is employed to measure interference by splitting a beam of light into two arms (sample and reference). Light back-reflected from a mirror in the reference arm and reflectors within the sample are recombined causing interference that can be detected. The interference results in fringes across the spectrum of light with the frequency of the fringes scaling with the depth of the reflector (the higher the frequency the deeper the reflector).

To enable intravascular imaging, the sample arm of the interferometer becomes a catheter that can be inserted into the vasculature. A typical catheter consists of a single-mode optical fiber followed by a grin lens and a microprism or mirror to direct light toward the sample [1]. The catheter is housed within a torsion cable, which is rotated to produce the standard image as shown in the middle panel of Fig. 1. By pulling back the catheter while rotating 3-D images of the lumen can be produced. LightLab produced the first commercial catheter for intravascular imaging. The ImageWire^{TM} catheter has a diameter of 0.019", a lateral resolution of 40 μm, and a maximal scan diameter of 6.8 mm. LightLab's new Dragonfly^{TM} catheter for their C7-XR FD-OCT system has increased the pullback speed to 25 mm/s, the rotation speed to 100 revolutions/s, and increased the scan diameter to 11 mm. The increased pullback and rotation speed allow for a 55 mm segment to be imaged in 2–3 s. The Dragonfly^{TM} FD-OCT catheter is compatible with a conventional 0.014" angioplasty guide wire, designed for rapid-exchange delivery; the

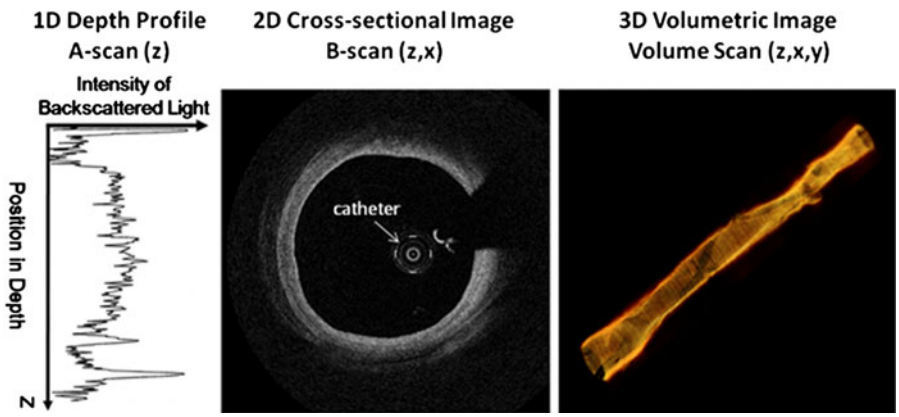

Fig. 1 OCT scanning schemes. The *left* panel shows a typical A-scan collected from a sample. The *middle* panel depicts a typical B-scan of a coronary vessel where the catheter has been rotated, thus scanning a cross-section of the vessel. The data is transformed into polar coordinates to accurately portray the circular structure of the vessel. The *right* panel illustrates volumetric imaging of a coronary vessel. To achieve 3-D imaging the catheter is pulled back as it is rotating tracing out a helical pattern

catheter has a distal diameter of 2.7 Fr and is compatible with 6 Fr guiding catheters.

Over the last several years there has been a paradigm shift in the basic approach to building OCT systems. Fourier domain OCT (FD-OCT) has been established as the preferred method for OCT imaging due to its increased sensitivity which can be used for imaging orders of magnitude faster [17–20]. The conventional setup or time domain OCT (TD-OCT) setup employed a scanning mirror in the reference arm to temporally observe the interference fringes a single point at a time, which wasted the light returning from other depths. In FD-OCT, an entire A-scan is detected simultaneously by observing fringes on the spectrum of light. Currently two methods exist to perform FD-OCT imaging as shown in Fig. 2 (swept-source OCT (SS-OCT) and spectral-domain OCT (SD-OCT)). In SD-OCT the reference arm is static, while a spectrometer in the detector arm disperses light onto a line scan camera. Each pixel on

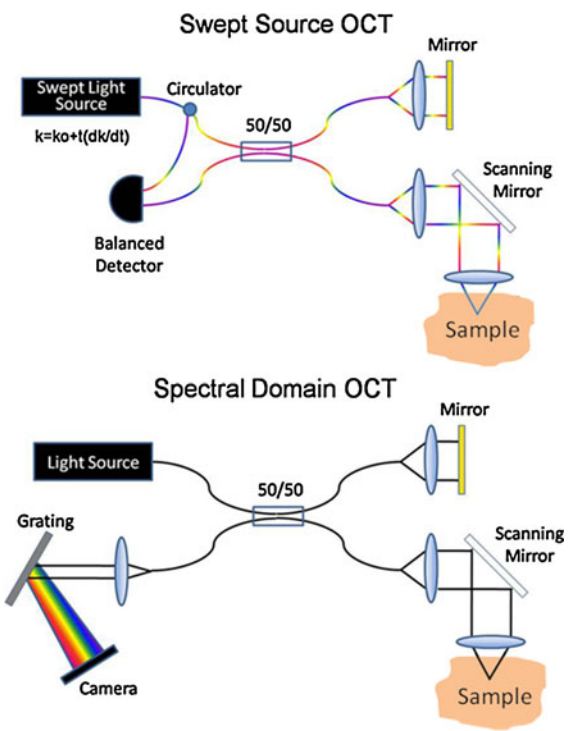

Fig. 2 SDOCT and SSOCT configurations. In both setups the reference arm is static. With SDOCT a spectrometer disperses light across a line scan camera. Modulations in the spectrum can be seen across the pixels of the camera. In SSOCT a swept source laser is employed and a photodetector captures modulations on the spectrum over time

the camera detects a portion of the spectrum. The camera limits the imaging speed with typical commercial systems imaging at 20–52 kHz line rates. SD-OCT is primarily used for ophthalmic imaging. With SS-OCT [15, 21, 22] sometimes referred to as optical frequency domain imaging [23] the reference is again static, but a swept source laser is employed. A swept source laser sweeps through its bandwidth as a function of time allowing only a small band of wavelengths to emit at any instant. A photodetector collects portions of the spectrum as a function of time. The sweep speed of the laser limits the imaging speed with typical commercial systems imaging at 16-50 kHz line rates. Currently, intravascular OCT employs a SS-OCT setup. FD-OCT has several disadvantages (autocorrelation artifacts, complex conjugate artifact and fall-off of the signal with depth) compared to TD-OCT, but the disadvantages are negligible in intravascular OCT imaging [1].

Equation 1 shows the math governing OCT imaging [17]. The first and second term signifies the light returning from the sample and reference arm of the interferometer,

$$P(k) = S(k)R_r + S(k)R_s + \int 2S(k)\sqrt{R_r R_s(\Delta l)}\cos(2k\Delta l)d\Delta l \qquad (1)$$

while the third term represents interference between the two arms of the interferometer. By removing the DC terms ($S(k)R_r$, $S(k)R_s$) from Eq. 1, the OCT image can be reconstructed from the third term. $S(k)$ is the spectral density of the source R_r and R_s are the reference and sample arm reflectivities, and k is the wavenumber ($\frac{2\pi}{\lambda}$, λ = wavelength), while Δl is the mismatch in path length between the sample and reference arms. Each reflector in the sample is at a set Δl with the reference arm and creates interference fringes at a single frequency across the optical spectrum (sampled evenly in wavenumber (k)). The greater the mismatch in length (Δl) or depth of the reflector in the sample arm the higher the frequency of the interference fringes across the spectrum according to the cos function in Eq. 1. The top three panels in Fig. 3 demonstrate increasing frequency of the spectral interference fringes on the spectrum with increasing depth of the reflector. The collected data is a superposition of the frequencies created by reflectors from the many depths within the sample (see

bottom panel of Fig. 3). By Fourier transforming the data the location and amplitude of the reflectors in the sample are identified.

In OCT imaging the axial (along A-scan) and lateral (along B-scan) resolutions are decoupled from each other. Axial resolution is inversely proportional to the bandwidth of the light source. For example, the broader the bandwidth of the light source the higher the axial resolution. Axial resolution can be estimated by Eq. 2, where λ_o represents the center wavelength of the light source and $\Delta\lambda$ is the full width half maximum (FWHM)

$$\text{axial resolution} = l_c = \Delta z = \frac{2\ln 2\,\lambda_o^2}{\pi \quad \Delta\lambda} \tag{2}$$

bandwidth of the source. FWHM bandwidth refers to the bandwidth of the source at half the maximum intensity. Under ideal conditions, an OCT setup utilizing a light source with a center wavelength of 1,300 nm and a bandwidth (FWHM) of 70 nm will result in an axial resolution of 10.6 μm in air. Axial resolution is measured by placing a mirror in the sample arm and determining the FWHM of the point spread function. Typical commercial OCT systems have axial resolutions of 10–15 μm.

Lateral resolution is determined by the spot size of the objective lens in the OCT system. Equation 3 can be used to estimate the spot size for a given focusing system.

$$\text{lateral resolution} = \Delta x = \frac{4\lambda}{\pi}\frac{f}{D} \tag{3}$$

D is the diameter of the light beam at the focusing lens and f is the focal length of the lens. λ is the central wavelength of the light source. Lateral resolution can be assessed by measuring the spot size of the focused light with an optical beam analyzer. The lateral resolution of an OCT system varies with depth and only achieves its highest resolution at the focus. The confocal parameter or depth of focus determines the axial range where the spot is increased less than $\sqrt{2}$

$$\text{confocal parameter} \cong \frac{\pi\Delta x^2}{\lambda} \tag{4}$$

times the spot at the focus (see Eq. 4). Δx is the lateral resolution at the focus. Unfortunately, there is

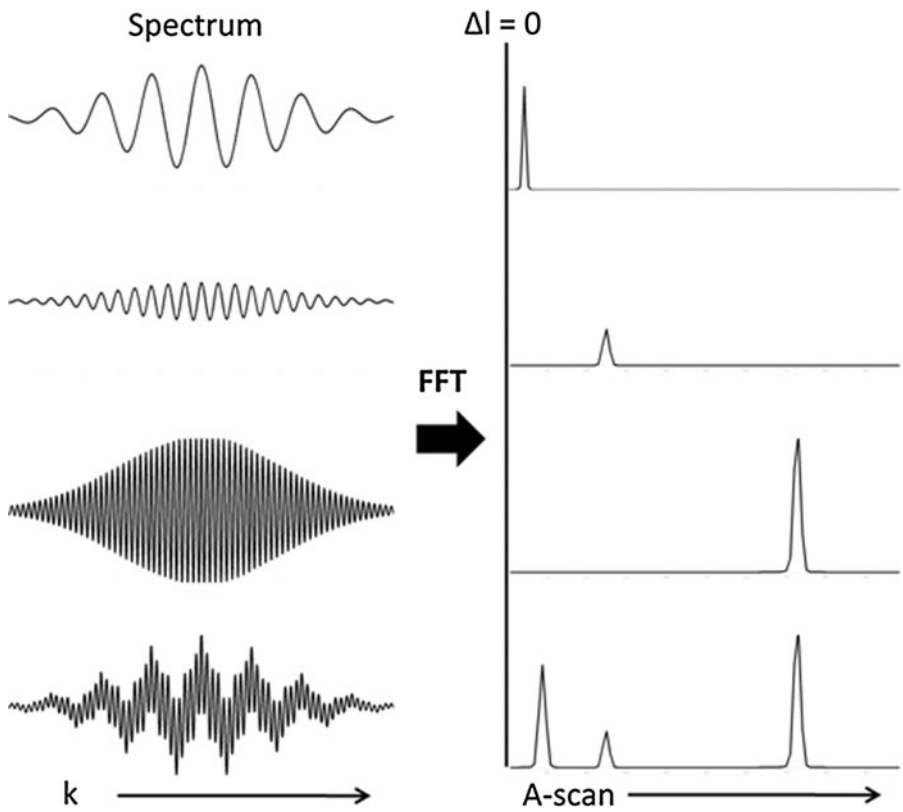

Fig. 3 FDOCT concept. Fringes on the spectrum are collected by sampling the spectrum even in wavenumber (k) and then Fourier transforming the data to determine the depth and amplitude of the reflector in the sample. On the left are collected spectrum with the corresponding A-scan on the right after the fast Fourier transform (FFT) has been applied. The *top* three spectrum and A-scans demonstrate that the further the reflector from zero pathlength match ($\Delta l = 0$) the higher the frequency on the spectrum. The *bottom* spectrum is a superposition of the frequencies created by reflectors from the multiple depths within the sample as shown in the corresponding A-scan

a tradeoff between lateral resolution and depth of focus as higher numerical aperture (NA) objectives lead to higher resolution at the focus, but the resolution drops off more quickly. Therefore, image quality is good over a shorter depth range. Numerical aperture refers to a range of angles that a lens can emit or collect.

Measuring the sensitivity of an OCT system is an important metric to determine the quality of the imaging system. Equation 5 gives the sensitivity for an FD-OCT system [17]. Here,

$$\text{Sensitivity}(\text{dB}) = 10 * \log\left(\frac{\rho S R_s \Delta t}{2e}\right) \quad (5)$$

shot noise limited detection has been assumed. S is the source power, R_s is the sample arm reflectivity, ρ is the photodetector responsivity, e is the charge of an electron, and Δt is the integration time of the camera or the sweep time of the swept source. Typical OCT systems operate with an sensitivity slightly above 100 dB. Along with shot noise images may also suffer from laser intensity noise and noise from the data acquisition card.

OCT image acquisition

The adoption of intracoronary OCT imaging in clinical practice was hampered by the fact that infrared light cannot penetrate blood. Therefore, unlike intravascular ultrasound (IVUS) OCT requires clearing or flushing of blood from the lumen [5, 24–26]. This draw-back particularly affected TD-OCT acquisition as the moderate pull-back speed of this first generation OCT imaging system severely limited the size of the region that could be imaged during clearing or flushing of blood. Nonetheless, Jang et al. [13] with their pioneering work, imaged short coronary segments with intermittent 8–10 cc saline flushes through the guiding catheter. Jang et al. used a noncommercial TD-OCT system capable of imaging at 4–8 frame/s with an axial resolution of 13 μm. Later on, the two automated techniques of OCT acquisition, that are currently used, were set up.

The occlusive technique requires coronary blood flow interruption that is obtained by a gentle inflation with an occlusion balloon proximal to the imaged segment. During occlusion a crystalloid solution, usually Ringer's lactate, is flushed through the end-hole of the balloon catheter at a flow rate of 0.5–1.0 ml/s. The vessel occlusion time should be adjusted according to patient symptoms and severity of ECG changes (QRS duration and QT prolongation) with the infusion set to stop automatically after a maximum of 35 s to avoid hemodynamic instability or arrhythmias [27, 28]. A power injector is recommended for injection of the flush solution at a constant rate. Multiple pull-backs can be performed to accomplish complete lesion assessment. This occlusive technique has some limitations: (1) a balloon-vessel size mismatch may occur and this leads to inadequate clearing of the lumen with insufficient image quality, (2) ostial and proximal lesions (<15 mm from ostium) cannot be imaged due to the presence of the occlusive balloon.

The non-occlusive technique, that has been developed later, does not require proximal balloon occlusion. A standard intracoronary guide wire is generally used to cross the target lesion and to enable insertion of an over-the-wire intracoronary probe with an inner lumen compatible with the diameter of the OCT probe. The guide wire is then switched with an image wire and pull-back is performed at the highest available speed during simultaneous infusion of a viscous iso-osmolar solution through the guiding catheter.

One infusion protocol requires manual injection of a commercially available contrast agent (Iodixanol 320, Visipaque™, GE Health Care, Ireland) through the guiding catheter at an infusion rate between 1 cc/s and 3 cc/s, based on the run-off of the artery and the on-line assessment of the OCT image quality. This contrast agent is recommended both for its low arrhythmogenic potential and for its high viscosity, the latter helpful to prolong imaging time. Large series show that the blood can be completely displaced from the artery during the entire acquisition period [29, 30]. Technical developments described below have the potential to drastically reduce the imaging time so that a very short hand- or power-injection will suffice for optimal image acquisition. Due to its ease and safety, the OCT non occlusive technique is an alternative approach favoured by some investigators.

As compared to TD-OCT, FD-OCT enables one to image orders of magnitude faster, which increases the utility of OCT in intracoronary imaging by being able to image a much larger segment of the coronary

lumen and reduce motion artifacts. For example, the C7-XR FD-OCT imaging system from LightLab allows for a maximum pullback speed of 25 mm/s and a acquisition speed of 50,000 A-scans/s compared to 4,000 A-scans/s with the M2x TD-OCT system. The increased speed also allows higher spatial sampling by allowing an increased number of A-scans in a single image. For example, the LightLab TD-OCT system used 200 A-scans per frame compared to 500 A-scans used per frame with the FD-OCT system. The increase in A-scans allows one to see structures with more clarity. The increased speed of FD-OCT has significantly improved both the quality and ease of use of OCT in the catherization laboratory [31–33].

The technique of acquisition for FD-OCT has been optimized and follows the non occlusive method of acquisition developed for TD-OCT. Contrast solution, due to its viscosity, can displace blood cells for a sufficient period of time as to be able to record OCT images in a certain coronary segment. Obviously the fact that FD-OCT images can be obtained at a speed up to 25 mm/s enables the acquisition of long coronary segments in a very short time.

Using the LightLab FD-OCT system, the OCT probe is first positioned over a regular guide wire, distal to the region of interest. Identification of the pull-back starting point is a simple task as a dedicated marker identifies the exact position of the OCT beam, located 10 mm proximal to the marker itself. When the OCT catheter is positioned, and blood clearance is visually obtained distally through the contrast injection, the acquisition of a rapid OCT image sequence with fast pullback can be automatically commenced by injecting a bolus of solution through the guiding catheter, with the pullback speed set between 5 and 25 mm/sec. The infusion rate of contrast is usually set to 3–4 ml/s for the left coronary artery and 2–3 ml/s for the right coronary, but can be modified based on the vessel run-off and size. Most expert users advocate the use of automated contrast injection to optimize image quality. The pull-back can start automatically when blood clearance is distally recognized or can be manually activated. An acquisition speed of 20 mm/s enables the acquisition of 200 cross-sectional image frames over a 4–5 cm length of artery in 3.5 s with a total infused volume of 14 ml of contrast. This may represent a concrete advantage of FD-OCT for the use in percutaneous coronary interventions (PCI), allowing quick evaluation of the stent and of the landing zones, avoiding geographical miss. The FD-OCT pull-back speed is too fast to interpret the run during the acquisition but the recorded images are stored digitally and can be reviewed in a slow playback loop [34].

For both the LightLab TD-OCT and FD-OCT systems, accurate calibration is mandatory to take full advantage of the high spatial accuracy of the technology. The size of the OCT image is calibrated by adjusting the z-offset, the zero-point setting of the system. In the FD-OCT system, the calibration procedure is fully automated. To maintain accurate measurements, the z-offset must be readjusted prior to off-line analysis and monitored throughout the longitudinal segment [24].

The higher profile of the Dragonfly^{TM} FD-OCT catheter as compared to the first generation of the ImageWire may offer advantages and disadvantages. Naturally the crossing profile may limit the use in very stenotic segments. On the other hand, the higher profile of the catheter precludes extreme wire eccentricity as observed with the first generation. This results in less artifacts and out of focus images.

Previous experience with TD-OCT technology, either occlusive and non-occlusive, shows OCT acquisition to be safe and effective [24, 28]. Preliminary data on the safety for the use of FD-OCT technology are even more promising; in fact no ischemic ECG changes or arrhythmias develop during the short injection period. This is due to the marked simplification of the acquisition procedures and the consequent reduction in the required contrast volume [32, 35]. These preliminary data also indicate that FD-OCT is highly effective, as it can study longer segments with clear images compared to TD-OCT [32, 33]. As with TD-OCT, FD-OCT image quality depends on accurate methodology and proper guiding catheter engagement to optimize directional contrast flushing. OCT provides excellent differentiation between the vessel lumen and the arterial wall, facilitating the determination of lumen areas and volumes, and the depiction of stent struts with high accuracy [36, 37]. Furthermore, studies of quantitative measurements of lumen, stent and neointimal areas reveal a high reproducibility, primarily driven by the high resolution of the technology [33, 37].

Preliminary data from our group on the safety, and feasibility of FD-OCT have been obtained in 90

patients (114 OCT acquisitions). In all but 1 (99.1%) the procedure was successful: despite the high prevalence of imaged vessels with marked tortuosity and calcifications. The mean time of a FD-OCT pull-back (from the set up to the completion of the pull back) was 2.1 min and an average contrast volume of 49.4 ± 19.0 cc was specifically required for OCT assessment. No patients suffered contrast induced nephropathy and no major complications were recorded: only in one patient the image-wire negotiation led to a transient vessel spasm that was resolved with intracoronary administration of nitrates. During FD-OCT image acquisition no ischaemic ECG changes occurred and other major arrhythmias (ventricular tachycardia of fibrillation) were not observed [32].

Future concerns and developments

Further validation studies are needed to show that FD-OCT measurements of luminal areas and length of the analyzed segments can be obtained with high reproducibility. Unlike IVUS, OCT images have not been acquired using ECG gating, which is capable of acquiring cross sections in the same phase of the cardiac cycle, such as end-diastole [38]. Such a modality of acquisition or alternatively the adoption of a post labeling selection of a specific cardiac cycle phase, can therefore be applied to IVUS as to eliminate the systo-diastolic artifacts induced by coronary movement (sow-fish appearance) [38]. At the superb high pull-back speed (20 mm/s or more) of FD-OCT different portions of the imaged coronary segment will be acquired either in the systolic or diastolic phase. This may be an issue as IVUS studies showed that luminal area exhibit variations of about 5% during the cardiac cycle [39]. Reproducibility studies obtained during serial pull-back will show whether this draw-back will turn into a limitation for research studies and clinical applications of FD-OCT.

Current commercial OCT systems have not realized their maximum speed. As new swept lasers become commercially available, commercial systems can expect to increase imaging speeds several fold and ultimately be limited by the power needed on the sample to produce a good image. Resolution in commercial OCT units can expect to improve as ultra-broadband light sources become more portable. Also, Doppler OCT imaging may become an important tool to assess tissue perfusion [1, 40, 41]. Finally, image processing will play a role in enabling measurements and visualizations that are able to diagnose disease and be used to make treatment decisions. OCT is starting to realize its robust potential and is becoming a useful tool in intravascular imaging.

Conflict of interest None.

References

1. Drexler W, Fujimoto JG (eds) (2008) Optical coherence tomography technology and applications. Springer, Heidelberg
2. Huang D et al (1991) Optical coherence tomography. Science 254(5035):1178–1181
3. Fercher AF et al (2003) Optical coherence tomography—principles and applications. Reports Progress Phys 66:239
4. Bouma BE, Tearney GJ (eds) (2003) Handbook of optical coherence tomography. Marcel Dekker, Inc., New York
5. Regar E, Serruys PW, Van Leeuwen TG (eds) (2007) Optical coherence tomography in cardiovascular research. Informa Healthcare, London
6. Tearney GJ et al (1997) In vivo endoscopic optical biopsy with optical coherence tomography. Science 276(5321): 2037–2039
7. Tearney GJ et al (1996) Scanning single-mode fiber optic catheter-endoscope for optical coherence tomography: erratum. Opt Lett 21(12):912
8. Rollins AM et al (1999) Real-time in vivo imaging of human gastrointestinal ultrastructure by use of endoscopic optical coherence tomography with a novel efficient interferometer design. Opt Lett 24(19):1358–1360
9. Yun SH et al (2007) Comprehensive volumetric optical microscopy in vivo. Nat Med 12(12):1429–1433
10. Xi J et al (2009) High-resolution OCT balloon imaging catheter with astigmatism correction. Opt Lett 34(13): 1943–1945
11. Tearney GJ et al (1996) Scanning single-mode fiber optic catheter-endoscope for optical coherence tomography. Opt Lett 21(7):543–545
12. Brezinski ME et al (1996) Optical coherence tomography for optical biopsy. Properties and demonstration of vascular pathology. Circulation 93(6):1206–1213
13. Jang IK et al (2002) Visualization of coronary atherosclerotic plaques in patients using optical coherence tomography: comparison with intravascular ultrasound. J Am Coll Cardiol 39(4):604–609
14. Jang IK, Tearney G, Bouma B (2001) Visualization of tissue prolapse between coronary stent struts by optical coherence tomography: comparison with intravascular ultrasound. Circulation 104(22):2754
15. Huber R, Wojtkowski M, Fujimoto JG (2006) Fourier Domain Mode Locking (FDML): A new laser operating regime and applications for optical coherence tomography. Opt Express 14(8):3225–3237

16. Jenkins MW et al (2007) Ultrahigh-speed optical coherence tomography imaging and visualization of the embryonic avian heart using a buffered Fourier Domain Mode Locked laser. Opt Express 15(10):6251–6267
17. Choma M et al (2003) Sensitivity advantage of swept source and Fourier domain optical coherence tomography. Opt Express 11(18):2183–2189
18. de Boer JF et al (2003) Improved signal-to-noise ratio in spectral-domain compared with time-domain optical coherence tomography. Opt Lett 28(21):2067–2069
19. Leitgeb R, Hitzenberger C, Fercher A (2003) Performance of fourier domain vs. time domain optical coherence tomography. Opt Express 11(8):889–894
20. Fercher AF et al (1995) Measurement of intraocular distances by backscattering spectral interferometry. Opt Commun 117(1–2):43–48
21. Golubovic B et al (1997) Optical frequency-domain reflectometry using rapid wavelength tuning of a Cr4 + : forsterite laser. Opt Lett 22:1704–1706
22. Choma MA, Hsu K, Izatt JA (2005) Swept source optical coherence tomography using an all-fiber 1300-nm ring laser source. J Biomed Opt 10(4):44009
23. Yun S et al (2003) High-speed optical frequency-domain imaging. Opt Express 11(22):2953–2963
24. Prati F et al (2010) Expert review document on methodology, terminology, and clinical applications of optical coherence tomography: physical principles, methodology of image acquisition, and clinical application for assessment of coronary arteries and atherosclerosis. Eur Heart J 31(4):401–415
25. Yabushita H et al (2002) Characterization of human atherosclerosis by optical coherence tomography. Circulation 106(13):1640–1645
26. Kume T et al (2006) Assessment of coronary arterial plaque by optical coherence tomography. Am J Cardiol 97(8): 1172–1175
27. Regar E, Prati F, Serruys PW (2006) Intracoronary OCT application: methodological considerations. In: Van Leeuwen TG, Serruys PW (eds) Handbook of optical coherence tomography. Taylor & Francis Books Ltd, London, pp 53–64
28. Tanigawa J, Barlis P, Di Mario C (2007) Intravascular optical coherence tomography: optimisation of image acquisition and quantitative assessment of stent strut apposition. EuroIntervention 3(1):128–136
29. Prati F et al (2008) From bench to bedside: a novel technique of acquiring OCT images. Circ J 72(5):839–843
30. Prati F et al (2007) Safety and feasibility of a new non-occlusive technique for facilitated intracoronary optical coherence tomography (OCT) acquisition in various clinical and anatomical scenarios. EuroIntervention 3(3): 365–370
31. Tearney GJ et al (2008) Three-dimensional coronary artery microscopy by intracoronary optical frequency domain imaging. JACC Cardiovasc Imaging 1(6):752–761
32. Imola F, et al. (in press) Safety and feasibility of Frequency Domain- Optical Coherence Tomography to guide decision making in percutaneous coronary intervention. EuroIntervention
33. Takarada S et al (2010) Advantage of next-generation frequency-domain optical coherence tomography compared with conventional time-domain system in the assessment of coronary lesion. Catheter Cardiovasc Interv 75(2):202–206
34. Barlis P et al (2009) A multicentre evaluation of the safety of intracoronary optical coherence tomography. EuroIntervention 5(1):90–95
35. Serruys PW et al (2009) A bioabsorbable everolimus-eluting coronary stent system (ABSORB): 2-year outcomes and results from multiple imaging methods. Lancet 373(9667): 897–910
36. Barlis P et al (2010) Quantitative analysis of intracoronary optical coherence tomography measurements of stent strut apposition and tissue coverage. Int J Cardiol 141(2): 151–156
37. Capodanno D et al (2009) Comparison of optical coherence tomography and intravascular ultrasound for the assessment of in-stent tissue coverage after stent implantation. EuroIntervention 5(5):538–543
38. von Birgelen C et al (1997) ECG-gated three-dimensional intravascular ultrasound: feasibility and reproducibility of the automated analysis of coronary lumen and atherosclerotic plaque dimensions in humans. Circulation 96(9): 2944–2952
39. Bruining N et al (1998) ECG-gated versus nongated three-dimensional intracoronary ultrasound analysis: implications for volumetric measurements. Cathet Cardiovasc Diagn 43(3):254–260
40. Yazdanfar S, Kulkarni M, Izatt J (1997) High resolution imaging of in vivo cardiac dynamics using color Doppler optical coherence tomography. Opt Express 1(13):424–431
41. Chen Z et al (1997) Noninvasive imaging of in vivo blood flow velocity using optical Doppler tomography. Opt Lett 22(14):1119–1121